Log spiral of revolution highly oriented pyrolytic graphite monochromator for fluorescence x-ray absorption edge fine structure

D. M. Pease, M. Daniel, J. I. Budnick, T. Rhodes, M. Hammes, and D. M. Potrepka
Physics Department, University of Connecticut, Storrs, Connecticut 06269

K. Sills and C. Nelson
Advanced Fuel Research, East Hartford, Connecticut 06118

S. M. Heald and D. I. Brewe
Argonne National Laboratory, Argonne, Illinois 60439

Anatoly Frenkel
Materials Research Laboratory, University of Illinois at Urbana-Champaign, Illinois

I. Grigorieva and A. Antonov
Optigraph Corporation, Moscow 117812, Russia

(Received 27 September 1999; accepted for publication 7 June 2000)

We have constructed an x-ray monochromator based on a log spiral of revolution covered with highly oriented pyrolytic graphite. Such a monochromator is used for obtaining x-ray absorption edge fine structure by the fluorescence method, and is particularly useful for measuring the fine structure of dilute element A in a concentrated matrix of element B, where B is to the left of A in the Periodic Table. Using the log spiral monochromator, we measure good Cr x-ray fine structure in an alloy of 1% Cr in a V matrix, whereas the corresponding spectrum is severely distorted by the V background if nonmonochromatized fluorescence is used. We also obtain excellent rejection of Mn fluorescence relative to Cr fluorescence in a $Cr_{80}Mn_{20}$ alloy, and can tune the monochromator such that the entire Mn step height is significantly smaller than the Cr x-ray absorption edge fine structure oscillations for this system. © *2000 American Institute of Physics.*
[S0034-6748(00)04109-5]

I. INTRODUCTION

X-ray background noise is one of the experimental problems that arise when one determines x-ray absorption edge fine structure (XAFS) of dilute atomic species using the fluorescence technique. Of particular interest is interference due to scattered radiation or fluorescence emission from elements other than the element of interest. Particularly troublesome is noise due to diffraction peaks, and also fluorescence from elements occupying a position on the Periodic Table just to the left $(Z-1)$ of the position of the atomic species of interest (Z). These noise sources contribute their own spectral features which interfere with the desired XAFS signal. In addition, fluorescence from $(Z-1)$ elements cannot be diminished by filters without seriously decreasing the signal from the desired element (Z), so that the standard ion chamber–filter–slit combination[1] cannot be used.

For specimens that are dilute in the element of interest, one gains increased detection figure of merit by efficient background removal, even if the total count rate is diminished thereby. Therefore, for dilute samples, the ion chamber–filter combination is sometimes replaced by a multidetecting element, energy-dispersive detector. For energy dispersive detectors, however, the total count rate one may obtain is often limited due to count pileup effects (saturation). The ability of multielement energy dispersive detector arrays to reject large background counts without saturation is increasing with development of more sophisticated electronics, and varies considerably between older and newer models of such detector arrays. In addition, multielement detector arrays are expensive and require liquid nitrogen cooling and ion pumping of the detector elements. We have as an alternative developed a log spiral[2] of revolution, graphite monochromator. This detector offers advantages in applications such as detecting XAFS in the presence of diffraction peaks, or in the presence of intense fluorescence from concentrated species which will saturate energy dispersive detectors.

A logarithmic spiral has the defining characteristic that all rays from a focal point meet the spiral at the same angle. In principle, one can therefore imagine a log spiral of revolution designed to monochromatize the fluorescence radiation emanating from a point focus in a fluorescence XAFS experiment. The ray bundle is not reflected to a true focus, but is concentrated in a region where photons can be detected by a nonenergy dispersive detector such as an ion chamber or an array of *p* doped-intrinsic-*n* doped (*PIN*) diodes. Because of a process recently developed in Russia whereby films of highly oriented pyrolytic graphite (HOPG) can be economically deposited on smooth surfaces,[3] such a monochromator becomes practical. The solid angle obtainable using a log spiral of revolution exceeds that obtainable with practical Johann crystal arrangements,[4] or Johannson bent crystals, and for the purpose of monochromatizing x rays, the fact that the log spiral does not focus to a point is not a disadvantage. Quite recently, Bakulin and Durbin have,

in a theoretical treatment, found that pyrolytic graphite curved to a logarithmic spiral has dramatically increased acceptance compared to standard monochromator designs. They predict that one can improve the collection efficiency per area of graphite over that attainable with sagittal focusing geometries by a factor of 200, while maintaining the intrinsic graphite energy resolution.[5]

For the initial log spiral that fits in our detector system, we have chosen the shape for detection of Cr K_α radiation. Cr is an important environmental pollutant,[6] and there is a need for developing improved ways to characterize its chemical speciation. Vanadium based alloys doped with Cr and Ti are of interest for proposed structural materials in fusion reactors, and there is interest in better understanding irradiation effects for these materials.[7] We show in this work that if data for 1% Cr in a V matrix is taken by standard methods using an ion chamber, the quality of the XAFS of the Cr edge for such systems will be so degraded by the V fluorescence that the data is unusable. Furthermore, V fluorescence from a sample concentrated in V will saturate energy dispersive detectors.

Our log spiral detector is shaped so that the Cr K_α line satisfies the Bragg condition for reflection by the (002) reflection of HOPG graphite, which corresponds to a planar spacing of 3.35 A. Calculations indicate that high quality ($\sim$0.4° mosaic spread) HOPG can reflect 50% of incident photons at the energy of the Cr K_α line,[8] although Moore points out that extinction can reduce the brightness.[9] Furthermore, Freund *et al.*, in a recent study of HOPG film reflectivity for different incident photon energies found that 200–300 μm HOPG can reflect 80% of the maximum allowed by a thick HOPG plate.[10]

The characteristics of the HOPG deposition process are such that thin layers (factor of 2 of 0.2 mm) can be molded onto smooth surfaces and will maintain a highly oriented, or low mosaic spread configuration. As the thickness of the layers increases, so does the mosaic spread. For Cr K_α radiation normally incident onto carbon, one absorption length is $\sim$1 mm. However, in practice, the effective penetration distance d is related to Bragg angle and total path length through the carbon such that for an absorption length of 1 mm, one has an attenuation length normal to the reflecting surface d of 0.17 mm. Thus, the manufacturing process is capable of applying HOPG layers, which are highly oriented, and of adequate thickness to give good intensity. (Although commercial *grafoil* is rather well oriented, our tests with a diffractometer show that the intensity one can attain using Cr K_α radiation using *grafoil* is less than that attainable with HOPG by roughly 2 orders of magnitude.)

II. DETECTOR GEOMETRY

The following discussion refers to Fig. 1. This figure represents half of a two dimensional slice through a log spiral of revolution with the Bragg angle chosen to reflect Cr fluorescence. The maximum solid angle which can be subtended by the log spiral depends on the minimum polar angle Φ_{MIN} at which the active area, covered with HOPG, begins. For the log spiral we have tested, the active area begins at

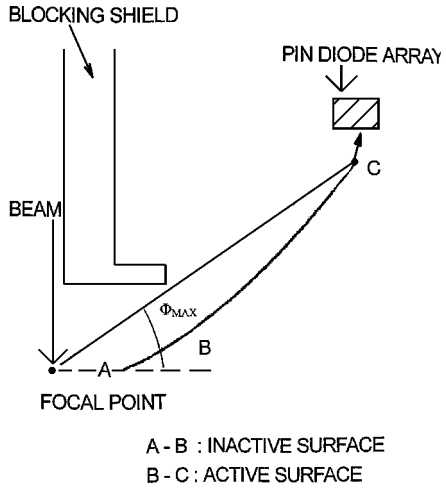

FIG. 1. Schematic drawing of a section through a log spiral manufactured for detecting Cr K_α. In the version of the log spiral discussed in this manuscript, the active (B–C) area of the surface (i.e., the surface covered with HOPG) begins at zero polar angle. The polar angle Φ shown corresponds to the maximum polar angle possible for Cr radiation if the active surface begins at zero polar angle.

zero polar angle. For this choice of minimum polar angle, the maximum polar angle Φ_{MAX} is about 30°, a limit which is set by the fact that the ray leaving the sample at zero polar angle and then diffracted by the HOPG is blocked by that HOPG surface which diffracts the $\sim$30° polar angle ray. This angular range, for a log spiral of revolution, corresponds to a solid angle of one third 2π, or 17% of 4π, which significantly exceeds the acceptance angle reported for the spherical Johann bent crystal shape of Hastings *et al.*,[4] and is comparable to the solid angle obtainable with typical multielement detectors. Were a similar log spiral detector to be manufactured for detecting Ti or Ca, this maximum solid angle would increase. For a log spiral made for any particular wavelength, if the minimum polar angle were chosen to be greater than zero, then the maximum allowable solid angle would also increase over that of the present design, and the emitted fluorescence would be on average less absorbed in the sample. We chose a 0° minimum polar angle for this version of the detector because this geometry gives the maximum solid angle per HOPG covering area, and is therefore the most financially economical.

We have constructed a log spiral with a scale such that there is a distance of 1.5 cm from the focus to the intersection between the zero polar angle ray and the spiral. For such a scale, we show in the following discussion that angular deviations from the ideal Bragg angle are within the 0.4° acceptance width of good HOPG if one assumes a sample plane normal to the incident beam and a 0.5 mm$\times$0.5 mm spot for the incident beam cross section. The relationship between spot size, geometrical scale, and angular resolution is discussed next.

We consider a flat sample, whose plane is perpendicular to the incident beam. Consider two ''ideal'' rays. These are an incident ray that strikes the sample exactly at the ideal focal point and a fluorescent ray leaving the ideal focal point and striking the HOPG at some point ''*p*.'' The emitted fluorescent ray leaves the sample surface at a polar angle of Φ

relative to that surface. Recall that for our present detector the maximum and minimum polar angles are 30° and 0°, respectively. Consider first the elongations of the beam spot, from the ideal focal point, which lie *in the plane* of an ''ideal'' incident and fluorescent ray. Let the spot elongation from the focal point be *d*, and the distance of the focal point from the HOPG be *D*. The angle α subtended by this spot elongation, at the HOPG surface, is given by the expression

$$\alpha = d \sin \Phi / D. \quad (1)$$

The angle α is also the deviation of the angle incident on the HOPG from the exact Bragg condition.

For the ray with minimum polar angle of zero, the exact Bragg angle condition is satisfied no matter how large the in plane elongation, since sin Φ is zero. For the largest (30°) polar angle ray, the ray strikes the log spiral at a distance *D* of about 57 mm, and for an 0.5 mm diam spot, the maximum deviation from the ideal Bragg angle is 0.125°, which is within the full width half maximum acceptance of 0.4° HOPG. For the border of a 1 mm spot, the deviation is 0.25°, which is just outside the full width half maximum (FWHM) of 0.4° HOPG.

Next, consider elongations of the beam spot *out of the plane* formed by a pair of ''ideal'' incident and fluorescent rays. For simplicity in visualization, imagine an out of plane beam spot elongation, relative to the focal point, which is perpendicular to the plane formed by the ''ideal'' incident and reflected rays. Consider a ray from this out of plane elongation, which strikes the HOPG at point *p*. The maximum elongation from the focal point is 0.25 mm for a 0.5 mm×0.5 mm spot and subtends a maximum angle with the HOPG at point *p* for the smallest value of *D*. The smallest *D* value is 15 mm for our detector, and corresponds to fluorescence rays with polar angles Φ equal to zero. The corresponding maximum out of plane angle Ψ the fluorescence ray subtends at the HOPG is equal to 0.95°. Then if η corresponds to the Bragg angle this out of plane ray makes with the HOPG, and θ corresponds to the Bragg angle subtended by the corresponding ''ideal,'' or in plane fluorescence ray, Thomsen has shown that one has the relationship[11]

$$\sin \eta = \sin \theta / \text{cosine}\, \Psi. \quad (2)$$

For the case of $\Psi = 0.95°$, η is nearly identically θ. For out of plane rays leaving the sample with polar angles exceeding zero, deviations of η from θ will be even less than for the 0° polar angle ray. One therefore deduces from Eqs. (1) and (2) that all rays are within the 0.4° FWHM acceptance width for a 0.5 mm×0.5 mm spot size and good quality HOPG, but some rays are just outside the FWHM for a 1 mm square spot size.

We now discuss briefly the geometrical considerations pertaining to the alignment of our monochromator. After the incident beam path is guided to be along the symmetry axis of the log spiral by a collimating button, there are two remaining adjustments which are used. First, the blocking shield shown in Fig. 1 is extended toward the sample until one attains the condition that no emitted fluorescence can directly go from the sample to the *PIN* diode array without first reflecting from the log spiral. Second, a micrometer drive can be used to move the sample surface toward or away from the incoming beam to tune the detector so that a maximum intensity is obtained for the x-ray fluorescence line of interest. For some tests, we remove the blocking shield so as to compare results using direct fluorescence onto the *PIN* diodes with results using only fluorescence rays reflected from the HOPG. At present, there is no shaft encoder on the micrometer drive, and during the course of testing the detector characteristics we found that for optimum performance, we needed to drive to the approximate optimum position of the sample using the micrometer drive, then fine tune by incrementing the micrometer position by hand, taking scans after each increment.

III. EXPERIMENTAL TESTS

Tests were done on a series of $V_xCr_{(1-x)}$ alloys and a $Cr_{80}Mn_{20}$ alloy. The alloys were melted in an arc melter, remelted several times, and polished flat. For the $V_xCr_{(1-x)}$ alloys, it must be kept in mind that the V K_β line corresponds to an energy only 13 eV from the energy of the Cr K_α line. The as emitted V K_β line has an intensity approximately 11% of that of the as emitted V K_α line.[12] Although the energy resolution of the HOPG is adequate for removing V K_α radiation from the Cr K_α signal, the V K_β line is not removed by the log spiral monochromator. (Energy dispersive detectors are also unable to remove the V K_β line when detecting Cr K_α.) We are able to make use of the V K_β line to help tune the micrometer sample positioner for samples dilute in Cr but concentrated in V, since the V_β energy position is so close to that of the Cr K_α line.

A. Preliminary measurements at the X-11 line of the National Synchrotron Light Source

For our first tests, a 1 cm wide, planar log spiral was manufactured, such that one half of the log spiral was covered with 0.2 mm HOPG and the other half with 0.4 mm HOPG. Tests were made on a $V_{0.5}Cr_{0.5}$ alloy, using a commercial energy dispersive detector for observing both direct fluorescence and fluorescence from the log spiral. We found that the 0.2 mm HOPG covering gave more intensity than did the 0.4 mm covering.

We then had machined a full log spiral of revolution plexiglas form using a computer assisted lathe. This form was covered with 0.2 mm of HOPG. An array of *PIN* diodes was also manufactured, using concepts and electronics discussed by Brewe *et al.*[13] and Bouldin *et al.*[14] The *PIN* diodes are 2 cm by 0.9 cm rectangles, and are laid end to end to approximate an annulus, positioned just beyond the HOPG covered region. The *PIN* diode array can intercept most, but not all the rays reflected from the HOPG. The *PIN* diodes are covered with several layers of aluminized mylar to prevent signal interference from visible light.

Initial experiments were done on the X-11 line of the National Synchrotron Light Source (NSLS). This beam is eventually to be commisioned for sagittal focusing, but at present, we were forced to use an unfocused beam spot on the sample which was ~2 mm×0.5 mm, by using the smallest opening of the hutch slits. We found that the rejection of V relative to Cr was worsened if we attempted to increase

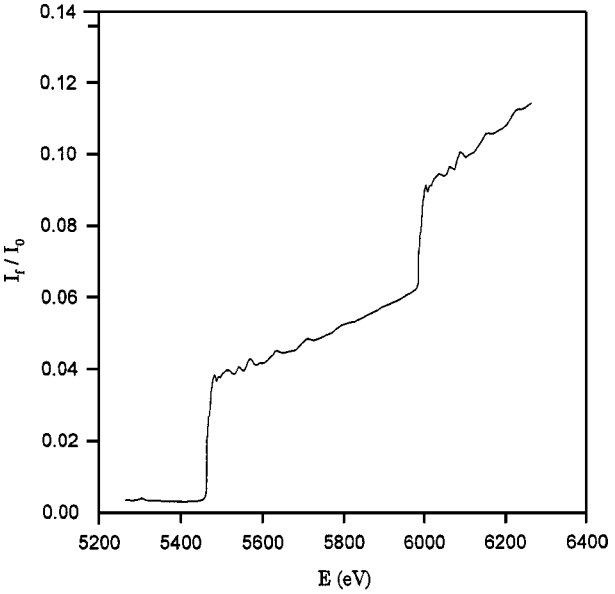

FIG. 2. EXAFS scan of both the V and Cr absorption edges of a $V_{0.5}Cr_{0.5}$ alloy using a standard ion chamber detector at the National Synchrotron Light Source.

intensity by using more of the beam. Estimated beam intensity with the 2 mm×0.5 mm spot was $\sim 1\times 10^9$ photons/s. Since the spot size was outside the ideal limit of acceptance by the HOPG in any case, we decreased sample self absorption and increased our intensity, somewhat further worsening the resolution, by tilting the sample at 45° around an axis which was the 2 mm beam width. Despite these nonideal conditions, we obtained promising preliminary results. Figure 2 shows an extended x-ray fine structure (EXAFS) scan on the $V_{0.5}Cr_{0.5}$ alloy, using a standard ion chamber detector. Figure 3 shows our corresponding EXAFS scan using the log spiral of revolution, averaging five data sets. The EXAFS of

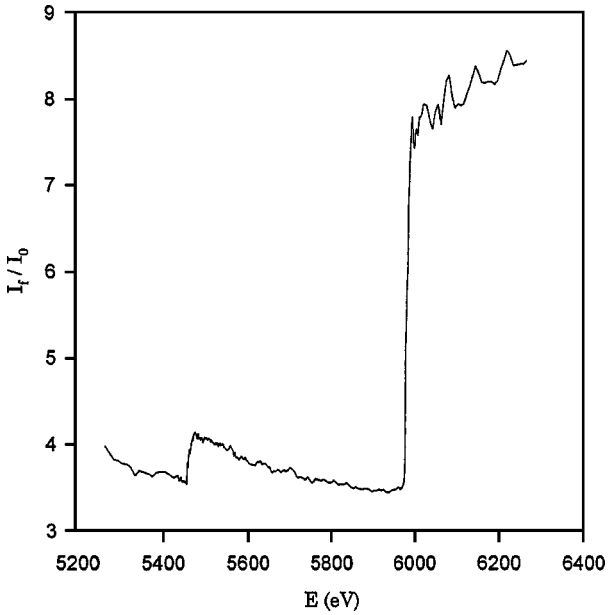

FIG. 3. EXAFS of a $V_{0.5}Cr_{0.5}$ sample using the log spiral detector at the National Synchrotron Light Source. Sample tilted at 45° relative to the beam with 2 mm×1 mm spot size as described in text. Average five scans.

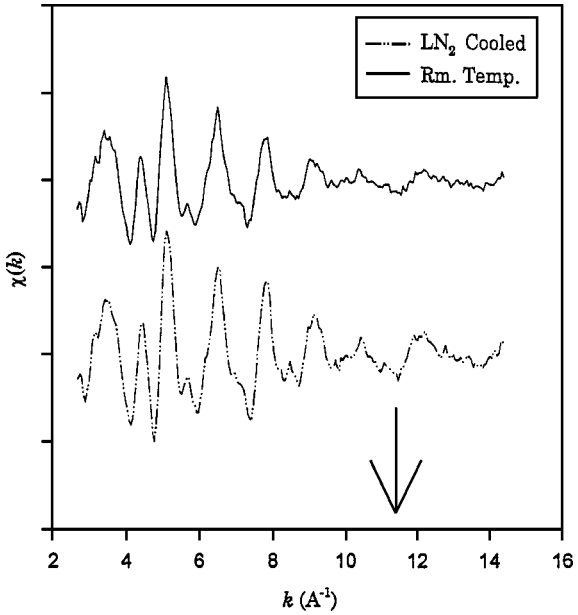

FIG. 4. (a),(b) EXAFS scan of $V_{0.99}Cr_{0.01}$ over energy regimes of both V and Cr edges; ion chamber data taken at the National Synchrotron Light Source. Background is subtracted. (a) Data taken at room temperature. (b) Data taken with liquid nitrogen cooling of the sample. The arrow indicates the position of the Cr edge threshold. The symbol k represents the wave number $2\pi/\lambda$ of the electron ejected by the absorption event, where λ is the deBroglie wavelength corresponding to the difference between the incident x-ray energy and the electron binding energy.

Cr is essentially the same for the two scans, but the V step height, relative to the Cr, is markedly reduced by the log spiral. The ratio of V to Cr step heights is reduced by a factor ~10 relative to the ion chamber result, but the ratio of Cr step height to pre-edge background is only enhanced by a factor of ~2. For data obtained later at the advanced photon source (APS), for which we used a smaller spot size and normal incidence of the incoming beam to the sample, the Cr step height to pre-edge background is enhanced by a factor of 16 relative to ion chamber data.

We carried out further experiments at the X-11 beam line to investigate the extent to which the Cr XAFS in $V_{0.99}Cr_{0.01}$ can be obtained by use of a standard ion chamber arrangement. Experiments were performed according to standard procedures using a commercial ion chamber used for detection of XAFS. Argon detector gas was used, as recommended, for detecting dilute species in this energy regime. Figures 4(a) and 4(b) show the XAFS including the V edge and the region of the Cr edge, with background subtracted to isolate the EXAFS oscillations. Figure 4(a) corresponds to data taken at room temperature and Fig. 4(b) corresponds to data taken at liquid nitrogen temperature. The arrow points to that energy which corresponds to the Cr edge threshold. It is evident that the Cr XAFS is completely overwhelmed by the V fine structure, and that the Cr data is unusable. We emphasize that the distortion of the Cr XAFS by the V XAFS is inherent to data taken on a dilute Cr in V sample using an ion chamber. Thus, Cr data obtained in this manner would remain distorted even if the counting statistics were to be markedly increased by use of a third generation synchrotron line or insertion devices.

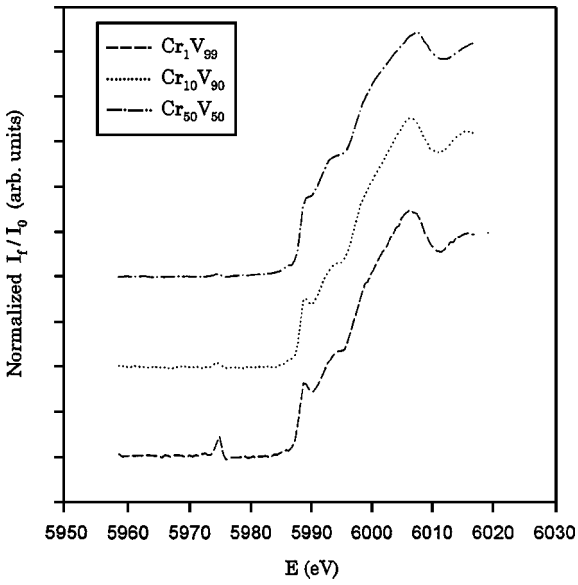

FIG. 5. XANES scans of the Cr K edge in a series of $V_xCr_{(1-x)}$ alloys taken with the log spiral of revolution, HOPG monochromator. The 1% Cr sample corresponds to the average of ten scans, the other samples are single scans. Data taken at the PNC-CAT line of the APS. Incident beam is normal to the sample surface with a 0.5 mm×0.5 mm incident beam spot. Background subtracted. There is a glich at about 5975 eV. The $Cr_{50}V_{50}$ curve is at the top, the $Cr_{10}V_{90}$ curve in the middle, and the Cr_1V_{99} curve is at the bottom.

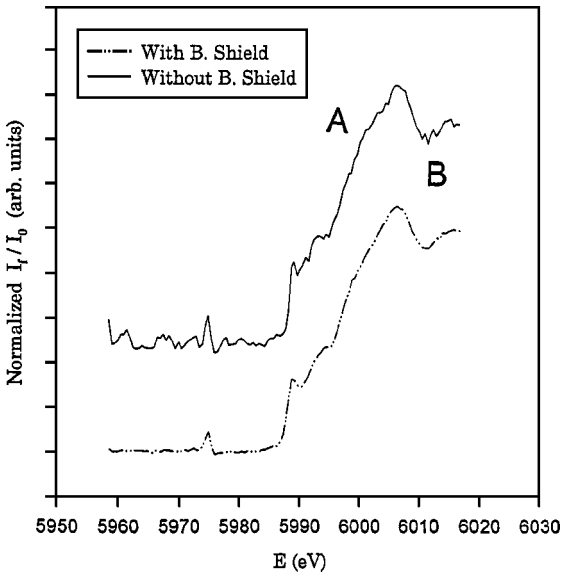

FIG. 6. XANES of Cr in $V_{0.99}Cr_{0.01}$, blocking shield out (top) vs blocking shield in (bottom). Background subtracted. Both data sets are ten averaged scans; identical beam conditions for both the blocking shield out and in conditions. Regions denoted by A and B are distorted in shape in the curve taken with blocking shield out.

B. Measurements at the advanced photon source

Experiments were done at the insertion device line of the Pacific Northwest Collaborative Access Team (PNC-CAT), at the APS. The beam does not at present have focusing, but the enhanced intensity over that available at the X-11 line at NSLS enabled us to use a 0.5 mm×0.5 mm beam spot, with 30% detuning, and a count rate of approximately 1×10^{11} photons/s at the Cr edge. The design projection is that, using a mirror, eventually this beam will attain still two orders of magnitude more intensity in this spot size. The presently available beam, in any case, is more than two orders of magnitude more intense for a given spot size than available for our experiments at NSLS. For the APS experiments we used the geometry for which the incident beam is normal to the sample plane, a geometry which corresponds to the best monochromator resolution.

There is one aspect of the X-11 line at the NSLS which is advantageous for these tests, relative to the PNC line at the APS. The X-11 line is a mature user facility for obtaining EXAFS fine structure, and is set up for scans which cover an extensive energy range. However, we were unable to obtain, at the PNC line, full EXAFS scans over two edges because of software limitations. The APS data are therefore used for comparisons of near edge scans taken for the Cr and V edges separately. Dark current subtractions are made for all data.

Figure 5 shows scans of the Cr edge in $V_{0.5}Cr_{0.5}$, $V_{0.9}Cr_{0.1}$, and $V_{0.99}Cr_{0.01}$, respectively, using the log spiral detector. The XAFS has had the background removed and the spectra are normalized. The spectra are similar, but show a removal of the fluorescence distortion observed for concentrated samples, as the concentration of Cr decreases. There may also be a sharpening of the x-ray absorption near edge spectra (XANES) due to alloying related electronic structure effects. The two most concentrated spectra correspond to single scans and the 1% Cr spectrum is the average of ten scans.

We made measurements at APS for the purpose of determining the ability of the HOPG log spiral to decrease the ratio of the V to Cr step heights in $V_xCr_{(1-x)}$ alloys. At the time these experiments were done, we had not yet discovered how extremely sensitive the optimum positioning of the sample plane was. Later experiments at the X-16 sagittally focused line at the NSLS made use of painstaking procedures for making this adjustment, whereas for the experiments at the APS we merely maximized the intensity with our micrometer drive. Nonetheless, if we denote by ''f'' the observed fraction of the step height ratio relative to the ratio of V to Cr in the sample, we obtained a value of f which was 0.13 for $V_{0.5}Cr_{0.5}$, 0.09 for $V_{0.9}Cr_{0.1}$, and 0.2 for $V_{0.99}Cr_{0.01}$. One should keep in mind that, neglecting small corrections due to air absorption and fluorescence yield, a minimum value of for f of $\sim$0.1 is to be expected based on the transmission of the V K_β line alone by the HOPG. For the $V_{0.5}Cr_{0.5}$ alloy the Cr step height to pre-edge x-ray background ratio can be compared to EXAFS data taken on the same alloy using an ion chamber as shown in Fig. 2, and is found to be enhanced by a factor of about 16.

The HOPG log spiral of revolution monochromator is an excellent device for obtaining dilute Cr XAFS in the presence of the XAFS of the V matrix. Figure 6 shows a comparison of Cr fluorescence from a 1% Cr in V alloy, obtained with the blocking shield in, versus the blocking shield out, and background subtracted. Identical beam conditions at the APS are used, on identical samples, using an average of ten scans. We emphasize that the *only difference* between these last two data sets is that, with blocking shield out, one adds direct fluorescence to the monochromatized signal obtained with blocking shield in place. The data obtained with the

blocking shield out results from fluorescence, some of which is monochromatized by the log spiral, and some of which reaches the *PIN* diodes directly. The data obtained with the blocking shield in is due to fluorescence, all of which is monochromatized by the log spiral. It is evident that use of the log spiral to monochromatize the data results in a significant improvement in data quality, and reduced distortion.

Finally, comparison of the normalized data using the log spiral, with the XAFS curves shown in Fig. 4, illustrates that use of the HOPG log spiral of revolution results in good data, whereas Cr edge data obtained by standard ion chamber techniques is unusable because of the inherent masking of the Cr edge by the V EXAFS.

C. Experiments at the X-16 line of the National Synchrotron Light Source

Experiments were done at the Lucent Technology/UIUC beamline X-16 C line of the NSLS. This line has sagittal focusing, produces a spot of diameter ~1 mm, and has an estimated intensity at the Cr edge of $\sim 1.3\times 10^{10}$ photons/s. This intensity is intermediate between the intensities of the X-11 line at the NSLS and the PNC line at the APS. This last set of experiments had as their primary purpose testing the ability of the log spiral to reject photons of higher energy than the Cr_α line. A sample of $Cr_{0.8}Mn_{0.2}$ was made and polished flat. This sample is sufficiently rich in Cr that one can readily tune to the approximately optimum sample position using the Cr K_α line, yet sufficiently rich in Mn to test for Mn K_α rejection. The ability to reject high energy photons is important for applications involving trace amounts of environmental Cr, and the separation of the Cr and Mn K lines is about the same as the energy separation of the Cr K_α line from incident beam scatter.

After our initial approximate alignment with the micrometer drive, we scanned the sample and found the Mn edge reduced relative to the Cr edge by about five times what would be expected solely on the basis of the 4:1 Cr to Mn ratio. However, we then began a series of experiments in which we incremented the sample position toward the incident beam, thus slightly increasing the Bragg angle, and scanning the edges after each scan. We attained a condition in which a small *negative* Mn step was observed on the Cr XAFS background. This observation is consistent with a situation in which, at energies above the Mn edge threshold, K shell excited Mn atoms have removed incoming photons from the channel which is available for exciting Cr K_α, and since the fluorescence is rejected by the log spiral, a small Mn edge is subtracted from the Cr XAFS. We then tried to tune the log spiral sample position to a point that just enough Mn fluorescence was transmitted to the *PIN* diodes to cancel the negative absorption jump due to Mn absorption. After several hours of trial and error, we generated the plot shown in Fig. 7. The position of the Mn edge is indicated, and at least by eye, no Mn edge is visible. We then moved the sample plane only ~1/8 in. further away from the incoming beam, past the optimum position for detection of Cr K_α, and into a region of sample position which would allow transmission of the Mn K_α line. The result is shown in Fig. 8. We

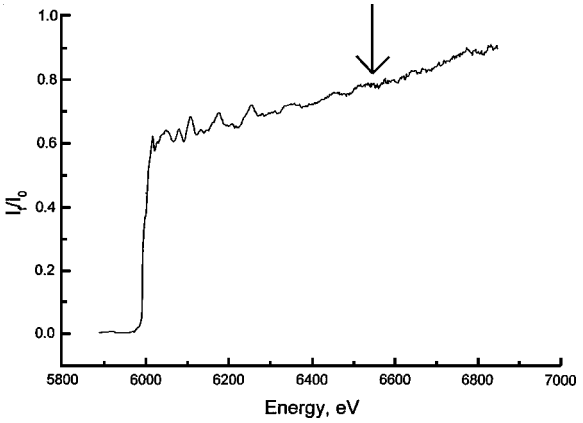

FIG. 7. EXAFS of both the Cr and Mn edges for a $Cr_{0.8}Mn_{0.2}$ alloy, with the sample position adjusted as described in the text to minimize the appearance of the Mn edge. The energy position of the Mn K edge is indicated by the arrow.

emphasize that Figs. 7 and 8 correspond to successive scans under identical beam conditions. These results show that if optimally aligned, and since there is no interfering K_β line, the ability of the logarithmic spiral of revolution, HOPG monochromator to reject high energy photons is excellent.

IV. DISCUSSION OF APPARATUS BRIGHTNESS

We conclude by discussing the brightness of the apparatus, and the possibilities for brightness improvement with future design changes. However, as shown in the discussion below, there are significant uncertainties in these considerations.

(1) Although we refer to the *PIN* diode array as ''annular,'' in actuality the array consists of rectangular diodes, 0.9 cm×2 cm, arranged in a circular trough cut in aluminum by a milling machine. The diodes are of good quality, but the shape was chosen because of availability. The 0.9 cm width would be just adequate to intercept the rays reflected by the log spiral if the diodes formed a perfect circular annulus, but in fact this is not the case. The diodes form an annulus approximated by rectangular segments. It is difficult to perform a quantitative measurement of intensity loss because of deviations from a perfect annular geometry, especially since

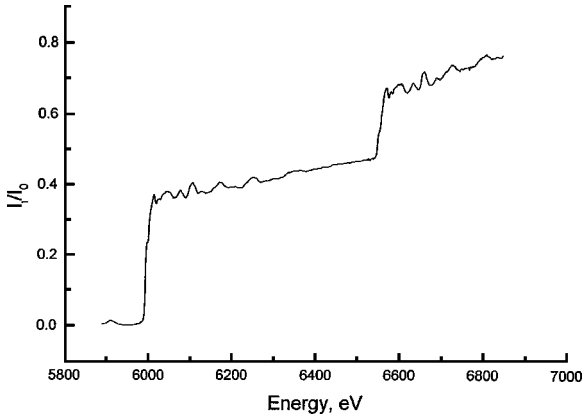

FIG. 8. EXAFS of both the Cr and Mn edges for a $Cr_{0.8}Mn_{0.2}$ alloy, all conditions the same as in Fig. 7 except the sample position is tuned slightly to the Mn edge and away from the Cr edge.

the diodes are hidden beneath layers of aluminized mylar. However, it is clear the diodes are failing to detect some fraction of photons coming from the HOPG. The intensity loss, due to using rectangular diodes to approximate an annular ring, is significant but probably less than a factor of 2.

(2) We have found that, for tests on the 50%Cr–50%V alloy, we gain a significant increase in intensity, with loss in resolution, by using a sample angled at 45° to the incident beam, rather than normal incidence. This intensity gain occurs despite a loss of half the solid angle of acceptance. For a normal incident beam, the log spiral as presently constructed has a significant portion of the solid angle positioned to accept rays corresponding to photons highly absorbed in the sample.

(3) The brightness of the HOPG is uncertain. Literature values are quoted in terms of Cu K energies for bulk specimens.[8,9] Freund *et al.* indicate the brightness can be less for films[10] than for bulk materials. One would expect the brightness to be less at the Cr than the Cu edges because of increased self absorption in the HOPG. Furthermore, the test of log spiral brightness was carried out at the X-16 line of the NSLS, which has a focused beam spot of 1 mm×1 mm, rather than the more desirable 0.5 mm×0.5 mm spot size at the PNC-CAT line of the APS.

Recognizing these uncertainties, we nevertheless compared the Cr step height for an alloy of 15% Cr in a matrix of 80% V and 5% Ti, with blocking shield in versus blocking shield out. We find the contribution to this step from the direct fluorescence to the *PIN* diodes is about three times the contribution from the log spiral. The direct fluorescence intensity is enhanced by a factor of roughly 4 relative to the intensity reflected off the HOPG because of the combined effects of: (a) self absorption in the sample when the low angle reflections of the HOPG are used, and (b) the fact that some of the rays reflected from the log spiral will pass through the plane of the *PIN* diodes at positions corresponding to annular radii greater or less than can be intercepted by the diode array. On the other hand, the *PIN* diodes lose relative to the log spiral by roughly a factor of 6 in total solid angle. The effects of relative intensity, solid angle, and *PIN* diode geometry combined would imply two thirds of 30% or 20% brightness of this HOPG for Cr radiation, using a 1 mm square beam spot. However, these estimates are quite approximate.

By extending the log spiral to accept rays with greater polar angles relative to the sample surface, while not depending on glancing emergent angle rays, the sample self absorption would decrease and the total solid angle would increase. Use of an annular ion chamber, rather than *PIN* diodes, would ensure that all rays reflected from the HOPG would correspond to detectable photons. A helium path would increase intensity at the Cr K edge by a factor of ~2. All these improvements could combine to enhance the intensity by a factor of ~8. We have demonstrated that the form of the detector as presently exists allows one to obtain XAFS on samples which cannot be studied by conventional techniques.

The log spiral of revolution is more ''tunable'' than one might suspect. By tuning to the V K_β line, we have successfully removed Ti background from the V edge in a $V_{0.5}Ti_{0.5}$ alloy. Of course, one suffers a ~×10 intensity loss relative to using a K_α line, but the data quality at the NSLS X-16 line is still excellent, and with intensities available at the APS, one could study dilute samples in this manner. We have also removed diffraction peaks from XAFS of a Ti–Cr–V reactor vessel alloy, for both V and Cr edges. These experiments will be fully reported elsewhere. Figure 8 suggests that the device could be used for samples containing Mn as well. A series of interchangeable log spirals of revolution could be manufactured for covering the transition metal 3d series for less expense than the cost of a multielement, energy dispersive detector.

ACKNOWLEDGMENTS

The authors are most grateful to John Nixon for helping the University of Connecticut by spending much time machining the logarithmic spiral of revolution shape with his company's computer assisted lathe for nominal charge, and to the Physics Department machine shop for other machining necessary to the project. They also appreciate the assistance at the Advanced Photon Source by Julie Cross and at The National Synchrotron Light Source by Kumi Pandya and Larry Fareria. This work was initially supported in part by the Department of Energy under Contract No. DE-FG05-94ER81861-A001, and subsequently supported by D.O.E. under Contract No. DE-FGO5-89-ER45385. The PNC-CAT project is supported by funding from the U.S. Department of Energy Basic Sciences, the University of Washington, Simon Fraser University, and the NSERC in Canada. The APS is supported by the U.S. DOE BES, Office of Energy Research, under Contract No. W-31-109-Eng-38. A.I.F. acknowledges support by DOE Grant No. DEFG02-96ER45439 through the Materials Research Laboratory at the University of Illinois at Urbana-Champaign.

[1] E. A. Stern and S. M. Heald, Nucl. Instrum. Methods **172**, 397 (1980).
[2] M. de Broglie and F. A. Lindemann, Compt. Rend. **158**, 944 (1914).
[3] A. A. Antonov, V. B. Baryshev, I. G. Grigorieva, G. N. Kulipanov, and N. N. Shcipkov, Nucl. Instrum. Methods Phys. Res. A **308**, 442 (1991); I. A. Grigorieva and A. A. Antonov, IEEE Nuclear Sci. Symposium and Medical Imaging Conference, Albuquerque, NM, 1997.
[4] J. B. Hastings, M. J. Perlman, P. Oversluizen, P. Eisenberger, and J. Brown, 5th Annual SSRL Users Group Meeting, SSRL Rept. No. 78-09 (1978).
[5] A. S. Bakulin and S. M. Durbin, Nucl. Instrum. Methods Phys. Res. A 441 (2000).
[6] Environmental Health Center, a division of the National Safety Council, 1025 Connecticut Avenue, NW, Suite 1200, Washington, DC 20036.
[7] A. van Veen, A. V. Federov, and A. I. Ryazanov, J. Nucl. Mater. 1400 (1998).
[8] C. J. Sparks, Metals and Ceramics Division, Oak Ridge National Laboratory, Annual Progress Report, ORNL-3970, p. 57 (1966).
[9] A. W. Moore, *Chemistry and Physics of Carbon* (Marcel Dekker, New York, 1973), Vol. 11, pp. 69–186.
[10] A. Freund, A. Munkholm, and S. Brennan, Proc. SPIE **2856**, 68 (1996).
[11] J. S. Thomsen, in *X-Ray Spectroscopy*, edited by L. V. Azaroff (McGraw-Hill, New York, 1974), pp. 26–132.
[12] *International Tables for X-Ray Crystallography* (Kynoch Press, Birmingham, 1962), Vol. III, p. 71.
[13] D. L. Brewe, C. E. Bouldin, D. M. Pease, J. I. Budnick, and Z. Tan, Rev. Sci. Instrum. **63**, 3298 (1992).
[14] C. R. Bouldin, R. A. Forman, and M. I. Bell, Rev. Sci. Instrum. **58**, 1891 (1987).